Development of Diamond Tracking Detectors for High Luminosity Experiments at the LHC, HL-LHC and Beyond

The RD42 Collaboration [1]

A. Alexopoulos[3], M. Artuso[20], F. Bachmair[24], L. Bäni[24], M. Bartosik[3], J. Beacham[13], H. Beck[23], V. Bellini[2], V. Belyaev[12], B. Bentele[19], P. Bergonzo[11], A. Bes[27], J-M. Brom[7], M. Bruzzi[4], G. Chiodini[26], D. Chren[18], V. Cindro[9], G. Claus[7], J. Collot[27], J. Cumalat[19], A. Dabrowski[3], R. D'Alessandro[4], D. Dauvergne[27], W. de Boer[10], S. Dick[13], C. Dorfer[24], M. Dunser[3], G. Eigen[30], V. Eremin[6], J. Forneris[15], L. Gallin-Martel[27], M.L. Gallin-Martel[27], K.K. Gan[13], M. Gastal[3], C. Giroletti[17], M. Goffe[7], J. Goldstein[17], A. Golubev[8], A. Gorišek[9], E. Grigoriev[8], J. Grosse-Knetter[23], A. Grummer[21], M. Guthoff[3], B. Hiti[9], D. Hits[24], M. Hoeferkamp[21], T. Hofmann[3], J. Hosslet[7], J-Y. Hostachy[27], F. Hügging[1], C. Hutton[17], J. Janssen[1], H. Kagan[13], K. Kanxheri[28], G. Kasieczka[24], R. Kass[13], M. Kis[5], G. Kramberger[9], S. Kuleshov[8], A. Lacoste[27], S. Lagomarsino[4], A. Lo Giudice[15], E. Lukosi[25], C. Maazouzi[7], I. Mandic[9], A. Marino[19], C. Mathieu[7], M. Menichelli[28], M. Mikuž[9], A. Morozzi[28], J. Moss[29], R. Mountain[20], S. Murphy[22], M. Muškinja[9], A. Oh[22], P. Olivero[15], D. Passeri[28], H. Pernegger[3], R. Perrino[26], F. Picollo[15], M. Pomorski[11], R. Potenza[2], A. Quadt[23], F. Rarbi[27], A. Re[15], M. Reichmann[24], G. Riley[25], S. Roe[3], D. Sanz[24], M. Scaringella[4], D. Schaefer[3], C. Schmidt[5], E. Schioppa[3], S. Schnetzer[14], S. Sciortino[4], A. Scorzoni[28], S. Seidel[21], L. Servoli[28], D.S. Smith[13], B. Sopko[18], V. Sopko[18], S. Spagnolo[26], S. Spanier[25], K. Stenson[19], R. Stone[14], B. Stugu[30], C. Sutera[2], M. Traeger[5], D. Tromson[11], W. Trischuk[16], C. Tuve[2], J. Velthuis[17], N. Venturi[3], E. Vittone[15], S. Wagner[19], R. Wallny[24], J.C. Wang[20], J. Weingarten[23], C. Weiss[3], N. Wermes[1], M. Yamouni[27], J. Zalieckas[30], M. Zavrtanik[9]

[1] Universität Bonn, Bonn, Germany, [2] INFN/University of Catania, Catania, Italy,
[3] CERN, Geneva, Switzerland, [4] INFN/University of Florence, Florence, Italy
[5] GSI, Darmstadt, Germany, [6] Ioffe Institute, St. Petersburg, Russia
[7] IPHC, Strasbourg, France, [8] ITEP, Moscow, Russia
[9] Jožef Stefan Institute, Ljubljana, Slovenia, [10] Universität Karlsruhe, Karlsruhe, Germany
[11] CEA-LIST Technologies Avancees, Saclay, France, [12] MEPHI Institute, Moscow, Russia
[13] The Ohio State University, Columbus, OH, USA, [14] Rutgers University, Piscataway, NJ, USA
[15] University of Torino, Torino, Italy, [16] University of Toronto, Toronto, ON, Canada
[17] University of Bristol, Bristol, UK, [18] Czech Technical University, Prague, Czech Republic
[19] University of Colorado, Boulder, CO, USA, [20] Syracuse University, Syracuse, NY, USA
[21] University of New Mexico, Albuquerque, NM, USA, [22] University of Manchester, Manchester, UK
[23] Universität Goettingen, Goettingen, Germany, [24] ETH Zürich, Zürich, Switzerland
[25] University of Tennessee, Knoxville, TN, USA, [26] INFN-Lecce, Lecce, Italy
[27] LPSC-Grenoble, Grenoble, Switzerland, [28] INFN-Perugia, Perugia, Italy
[29] California State University - Sacramento, CA, USA, [30] University of Bergen, Bergen, Norway

CERN-LHCC-2018-015 / LHCC-SR-005
27/05/2018

May 25th, 2018

[1] Contacts: H. Kagan (Ohio State), W. Trischuk (Toronto)

1 Introduction

The RD42 collaboration [1, 2] at CERN is leading the effort to develop radiation tolerant devices based on polycrystalline Chemical Vapor Deposition (pCVD) diamond as a material for tracking detectors operating in harsh radiation environments. Diamond has properties that make it suitable for such detector applications. During the last few years the RD42 group has succeeded in producing and characterising a number of devices to address specific issues related to their use at the LHC and HL-LHC [3]. Herein we present the status of the RD42 project with emphasis on recent beam test results and our proposed three year research plan. In particular, we review recent results on the stability of signal size on incident particle rate in diamond detectors over a range of particle fluxes up to 20 MHz/cm^2, on the radiation tolerance of CVD diamond, on the diamond work with ATLAS and CMS, on the results of 3D diamond detectors fabricated in pCVD diamond and on the work with diamond manufacturers. In addition, we present the details of our proposed 3 year program including milestones.

2 Rate Studies in pCVD Diamond

In order to study the stability of signal size on incident particle rate, RD42 performed a series of beam tests in the πM1 beam line of the High Intensity Proton Accelerator (HIPA) at Paul Scherrer Institute (PSI) [4]. This beam line is able to deliver 260 MeV/c π^+ fluxes from $\sim$5 kHz/cm^2 to $\sim$20 MHz/cm^2 in bunches spaced 19.8 ns apart.

Sensors made of CVD diamond material [5, 6] were tested in a tracking telescope [7] based on 100 μm $\times$ 150 μm CMS silicon pixel sensors [8] read out by the PSI46v2 pixel chip [9]. The diamond signals were amplified with custom-built front-end electronics with a peaking time of $\sim$6 ns, return-to-baseline in $\sim$16 ns and 550e noise with 2 pf input capacitance.The amplified signals were recorded with a DRS4 evaluation board [10] operating at 2 GS/s. The entire system was triggered with a scintillator that determined the timing of beam particles to $\sim$0.7 ns.

A series of cuts were applied: removing 60 s of triggers at the beginning of each run, triggers from heavily ionizing particles with saturated waveforms (mostly protons), calibration triggers, triggers in the wrong beam bucket, triggers with no tracks in the telescope and those with large angle tracks in the telescope. After applying this procedure all telescope tracks which project into the diamond fiducial region have a pulse height well separated from the pedestal distribution in the diamond i.e. the diamond is 100% efficient at all rates. The same procedure was applied to datasets from a range of beam fluxes and the resulting mean pulse height (in arbitrary units) versus rate is shown in Fig. 1a for negative diamond bias voltage and Fig. 1b for positive diamond bias voltage. The uncertainty on the data points in these plots includes both statistical and systematic sources. The systematic uncertainty was determined by assuming any deviations in pulse height for rates below 80 kHz/cm^2 was due to systematic effects. Thus the spread in the data points at a given rate indicates the reproducibility of the data. Fig. 1 indicates the mean pulse height in pCVD diamond detectors irradiated up to 4×10^{15} n/cm^2 does not depend on rate up to rates of 20 MHz/cm^2. RD42 is in the process of extending this study up to fluences of 10^{17} n/cm^2.

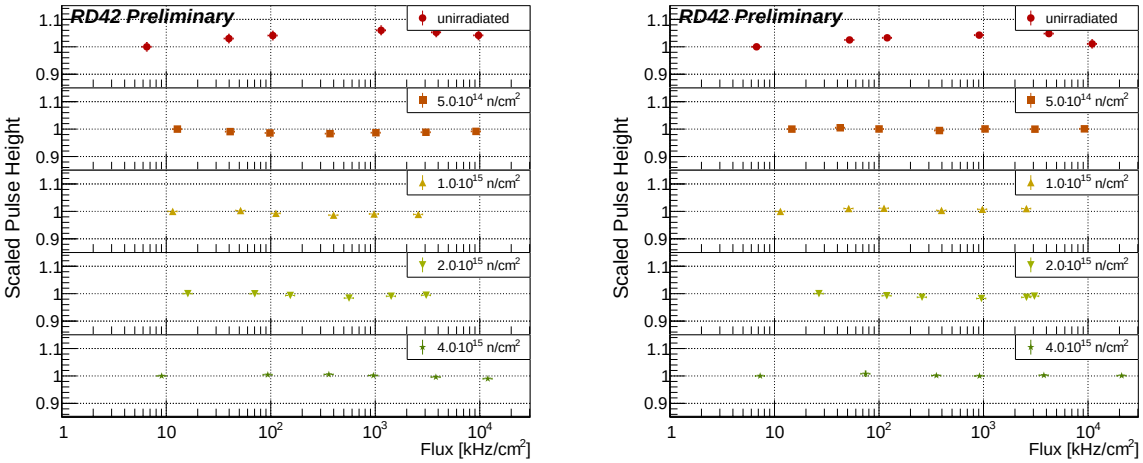

(a) (b)

Figure 1: The average pulse height versus rate for an un-irradiated and irradiated pCVD diamond pad detector at (a) -1000V and (b) +1000V bias. The data were taken by scanning up and down in rate multiple times. The pulse height units are arbitrary since the un-irradiated and irradiated detectors used different readout electronics. Electronics gain corrections and the relative gain correction for positive versus negative signals in the electronics is still being determined and has not been applied.

3 Radiation Tolerance Studies with CVD Diamond

Diamond samples, with a typical thickness of $\sim 500\mu$m, were cleaned with hot acid and etched with an oxygen plasma, metallized and tested with a source or in a beam test. Before being irradiated, they underwent "pumping" with a ^{90}Sr source to fill the intrinsic diamond traps, then the leakage current was checked to be below 10 nA. One single-crystal CVD (scCVD) diamond sample and three pCVD diamond samples were irradiated with 800 MeV protons at the Los Alamos Neutron Science Center (LANSCE) [11]. Two pCVD diamond samples were exposed to 70 MeV protons at the Cyclotron and Radioisotope Center of Tohoku University (CYRIC) [12] and two pCVD diamond samples were irradiated with fast reactor neutrons (>100 keV) at the Jožef Stefan Institute (JSI) TRIGA reactor [13]. After each irradiation, diamonds were metallized with a 50 μm pitch strip pattern with 25 μm wide strips on the growth side and a bias pad on the substrate side. Both patterns were produced with a standard photolithographic lift-off process. Each of the 128 strips was wire-bonded to an individual channel of a low noise front-end readout ASIC (eg. the VA2.2 [14]) to produce a diamond strip module. These modules were then tested with a 120 GeV/c hadron beam in the H6 secondary beam line of the CERN Super Proton Synchrotron (SPS). For all measurements, the diamond samples were biased with two polarities at $\pm$1V/μm and $\pm$2V/μm [7, 15]. The amplified signals were calibrated for the conversion from ADC to electrons and corrected for pedestal by subtraction and corrected for common mode noise. After these corrections, the common mode corrected noise was around 80e for each sample. The precise particle position in the diamond samples, approximately 2 μm, was determined with a high-precision telescope made of 8 planes of silicon strip detector plus a plastic scintillator trigger.

To estimate the damage induced by the radiation in diamond, a simple model with a linear dependence of the radiation induced traps with the fluence was used. This radiation damage model

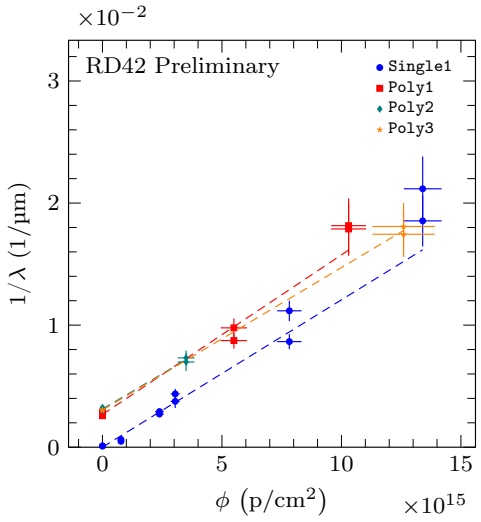

(a)

Particle Species	Relative Damage Constant, κ
24 GeV p	1
800 MeV p	1.85 ± 0.13
70 MeV p	2.5 ± 0.4
25 MeV p	4.5 ± 0.6
fast neutrons	4.5 ± 0.5
200 MeV π	2.5 - 3

(b)

Figure 2: (a) Inverse MFP ($1/\lambda$) as a function of 800 MeV protons fluence for 1 scCVD and 3 pCVD samples. For each fluence both HV polarities are shown. The statistical and systematic errors are added in quadrature. (b) Damage constant, κ, normalized to 24 GeV p, as a function of particle species and energy.

can be expressed in terms of the mean free path (MFP), which is the average distance traveled by electrons or holes between successive traps, as:

$$\frac{1}{\lambda} = \frac{1}{\lambda_0} + k\phi \tag{1}$$

where k is the radiation damage constant that is extracted with a fit to data for each CVD diamond sample. The initial MFP, λ_0, accounts for the inherent defects present in the pCVD samples and is measured before the irradiation with a ^{90}Sr source, whereas the MFP, λ, is derived from the average measured pulse heights from MIPs in a beam test [7, 15]. To evaluate the MFP from the measured pulse heights we assume that the MFP of electrons and holes is the same. The radiation damage constant depends upon the energy and irradiation particle (protons, pions or neutrons). Fig. 2a illustrates how the radiation damage constant was determined for the 800 MeV proton data. A similar procedure was used to extract the damage constant for 70 MeV protons as well as for the fast neutrons. The parallel slopes for pCVD and scCVD diamond samples in Fig. 2a indicate that both CVD materials are affected by the same radiation damage mechanism. The MFP measurements can be compared to those previously measured with 24 GeV protons [16, 17] by re-fitting that data [7, 15]. To do this, the fluences are scaled by:

$$\phi_{eq} = \kappa(\phi_i + \phi_0) \tag{2}$$

where κ is the relative radiation damage constant, summarised in Table 2b, defined as

$$\kappa = \frac{k_i}{k_{24GeVp}} \tag{3}$$

In this scaling, ϕ_0, is the equivalent fluence of the initial MFP, λ_0, of pCVD diamonds defined as:

$$\phi_0 = \frac{1}{\lambda_0 k_i}. \tag{4}$$

All the measured MFP as a function of the 24 GeV protons equivalent fluences are shown in Fig. 3a and are in good agreement with the simple radiation damage model.

The signal charge collected by the diamond device is proportional to the number of electron-hole pairs created as well as to the distance they travel under the applied electrical field. The width of the Landau distributed collected signal charge is related to the uniformity of the material. A reasonable figure of merit for the diamond devices is represented by the ratio, f, of the full-width-half-maximum divided by the most probable value of the Landau distributed collected signal charge. The measured figure of merit f versus the fluence for the pCVD and scCVD for 800 MeV proton fluences are shown in Fig. 3b indicating the interesting relationship between scCVD and pCVD material.

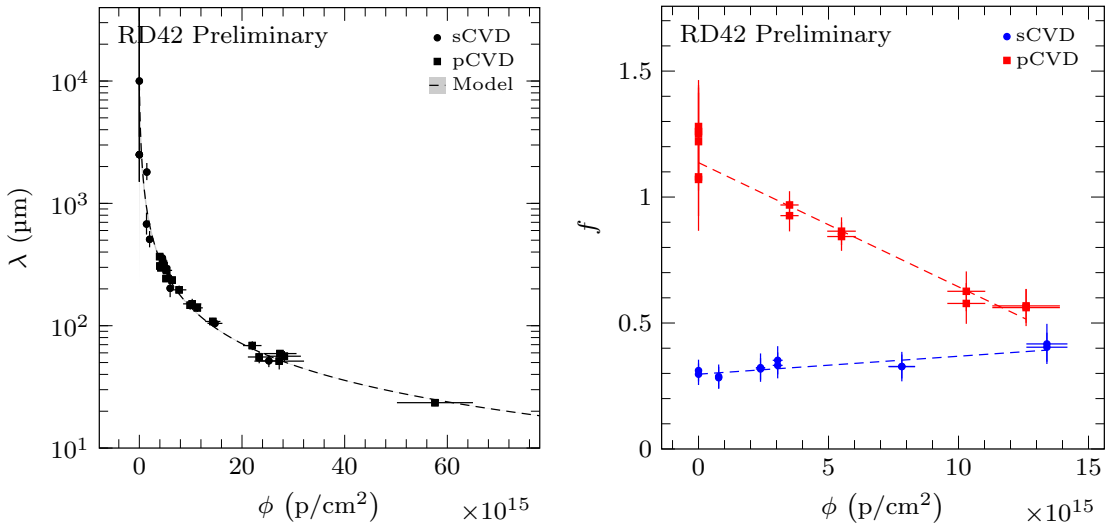

(a) (b)

Figure 3: (a) Measured MFP (λ) as a function of 24 GeV proton fluence compared to the radiation damage model (dotted curve) [15]. (b) Signal response figure of merit f for pCVD and scCVD samples as a function of 800 MeV proton fluence along with linear fits to pCVD (red line) and scCVD (blue line) data [15].

4 Status of the Collaboration with CERN/LHC Users

The RD42 group collaborates with the CERN/LHC users to enable their use of CVD diamond. Two recent examples of our successful coordination efforts with ATLAS and CMS are detailed below.

4.1 The ATLAS Diamond Beam Monitor

The startup of the LHC in 2015 brought a new milestone for diamond detector development when the first planar pCVD diamond pixel modules were installed in the ATLAS experiment [18]. The ATLAS Diamond Beam Monitor (DBM) [19] was designed to measure the instantaneous luminosity, the background rates and the beam spot position. For this project, RD42 provided diamond preselection, surface processing, metalization and the development of a compatible bump bonding process. A single DBM module consists of an 18 mm $\times$ 21 mm pCVD diamond 500 μm thick instrumented with a FE-I4 pixel chip [20]. The 26,880 pixels are arranged in 80 columns on 250 μm pitch and 336 rows on 50 μm pitch resulting in an active area of 16.8 mm $\times$ 20.0 mm. This fine granularity provides high precision particle tracking.

The ATLAS DBM uses diamonds with a charge collection distance (the average distance an electron-hole pair move apart under the influence of the applied electric field) of 200-220 μm at an applied bias voltage of 500 V. Three telescopes each with 3 diamond DBM modules (plus 1 telescope with silicon sensors) mounted as a three layer tracking device were installed inside the pixel detector services on each side of the ATLAS interaction point at 90 cm $< |z| <$ 111 cm, $3.2 < |\eta| < 3.5$ and at a radial distance from 5 cm to 7 cm from the center of the beam pipe. The modules are inclined at 10° with respect to the ATLAS solenoid magnetic field direction to suppress erratic dark currents [21] in the diamonds. The ATLAS DBM data-acquisition system is shared with the ATLAS IBL [22]. After initial installment, data were collected in the July 2015 run. These data have been analyzed and the first results of the ATLAS DBM tracking capabilities are shown in Fig. 4. A clear separation between background particles from unpaired bunches (open circles) and collision particles from colliding bunches (filled circles) is observed. After two electrical incidents in 2015 with consequent loss of several silicon and diamond modules, the DBM has now been re-commissioned and is in operation.

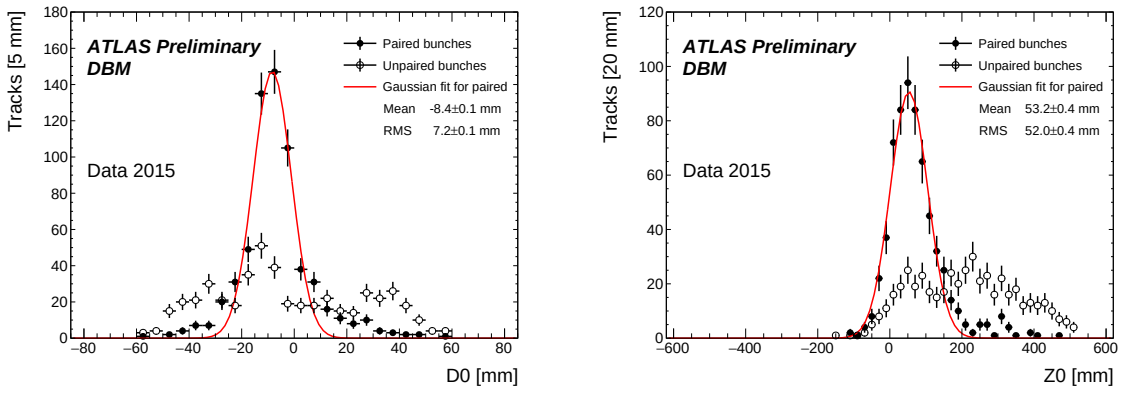

(a) (b)

Figure 4: (a) Radial distance and (b) longitudinal distance of of the projected particle tracks closest approach to the interaction point recorded by a single DBM telescope with preliminary alignment.

4.2 The CMS BCM1F Upgrade

In 2017 CMS installed a modified version of the BCM1F with 10 pCVD and 4 scCVD diamonds. Preselection, surface processing and metalization was performed by RD42. Diamond data from the selection process showed excellent HV stability which was the main concern of CMS. The devices were commissioned by Van der Meer scan and produced good luminosity measurements after initial installation. In 2017 the devices were exposed to 8 fb^{-1} of proton-proton collisions. The scCVD devices showed quick degradation, as expected, losing 60% of the charge relative to the test pulse signal while the pCVD devices remain stable with respect to the test pulse. In every LHC fill, a short Van der Meer-like scan (emittance scan) was performed and used to obtain a crude σ_{vis} for the ongoing monitoring of stability. σ_{vis} was tracked over many fills to measure detector stability, a measurement at different pile-up reveals potential non-linearities. Over the course of a fill a 2-3% change in σ_{vis} was observed; over the year-long data taking a 10% decrease in σ_{vis} was observed. The observed decreases include effects from optical readout degradation due to radiation damage, filling scheme and sensor stability. The BCM1F, corrected by emittance scan results produced a highly reliable luminosity measurement for CMS. Compared to other luminometers, the BCM1F stability over the year long period was $\sim 2\%$.

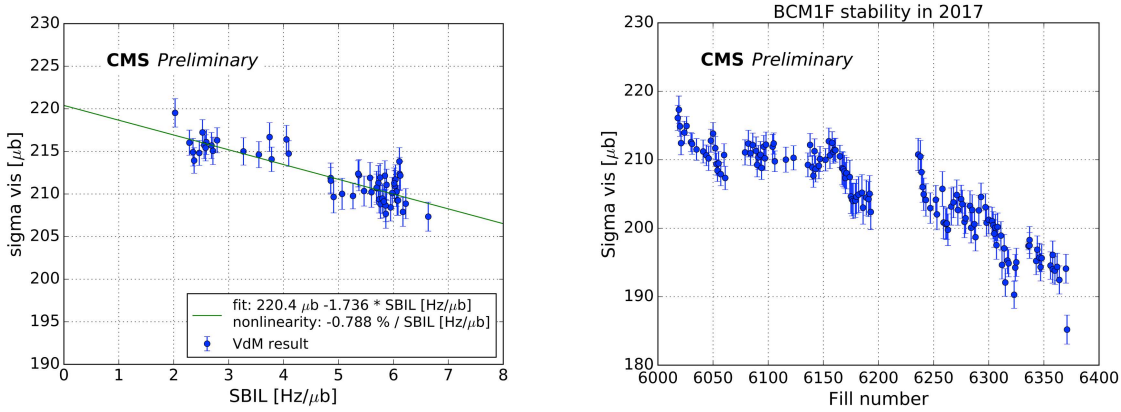

(a) (b)

Figure 5: (a) σ_{vis} during a single fill and (b) during the 2017 data taking period.

5 3D Diamond Pixel Detectors

3D sensors with electrodes in the bulk of the sensor material were first proposed in 1997 [23] in order to reduce the drift distance of the charge carriers to much less than the sensor thickness. In order to achieve this goal a series of alternating $+$ and $-$ electrodes perpendicular to the read out face were created in the bulk detector material. This idea is particularly beneficial in detectors with a limited mean free path such as trap dominated sensor materials like heavily irradiated silicon and pCVD diamond where the observed signal size is related to the mean free path divided by the drift distance. Under these circumstances one gains radiation tolerance (larger signals) by keeping the drift distance less than the mean free path. With this geometrical structure, charge carriers drift inside the bulk parallel to the surface over a typical drift distance of 25-100 μm instead of perpendicular to the surface over a distance of 250-500 μm.

In 2015 RD42 published results of a 3D device fabricated on an scCVD diamond [24] showing that the 3D structure works in diamond. In 2016 RD42 fabricated and tested the first 3D device in pCVD diamond [25]. The electrodes in the bulk of the pCVD diamond 3D device were fabricated with lasers as described in [24]. The bias electrodes were placed at the 4 corners of the cubic cells and the readout electrodes were placed in the middle of the cells. This pCVD device was shown to collect more than 75% of the deposited charge which translates in more than a factor of two more charge than a planar diamond strip detector fabricated on the same pCVD diamond.

In 2017 RD42 successfully constructed the first pCVD diamond 3D pixel detector with 50 μm $\times$ 50 μm cells. This pixel device was designed to be read out with the RD53 pixel readout chip [26] that is not yet available. In order to read this device out with an existing pixel readout chip a small number of cells were ganged together to match the pitch of the pixel readout chip. RD42 is proceeding to make 3D diamond pixel devices compatible with both the CMS pixel readout chip (3 $\times$ 2 ganging) and the ATLAS pixel readout chip (1 $\times$ 5 ganging). The first 50 μm $\times$ 50 μm pCVD diamond 3D pixel device with 3 $\times$ 2 ganging was bump-bonded using the CMS pixel readout chip.

This first diamond 3D pixel device was tested during the August 2017 beam test at PSI at a single voltage and with rates ranging from 7 kHz/cm^2 to 7 MHz/cm^2. During the initial lab test it was discovered that the bump bonding had a small issue in one corner. We decided to take data with the device rather than try to repair this small bump bonding issue. Fig. 6a shows the preliminary efficiency as a function of xy position for every cell in the device with a 1500e pixel threshold. The red box marks the fiducial region used to measure the hit efficiency. Fig. 6b shows the hit efficiency in the fiducial region with the 1500e pixel threshold as a function of time during an up-down scan of incident particle rates from 7 kHz/cm^2 to 7 MHz/cm^2 and back to 7 kHz/cm^2. The overall measured efficiency was 99.2% and no change in efficiency as a function of rate was observed. The corresponding efficiency for a planar silicon CMS pixel detector in this test was 99.7% with no change in efficiency as a function of rate. The slight loss of efficiency (0.5%), assuming it holds through the completion of the analysis, is most likely due to charge loss in the column electrodes. This explanation will be tested by measuring the efficiency as a function of tilt angle with respect to the incident beam during the 2018 test beams at CERN.

6 Development and Characterization of pCVD Diamond

Over the years, the RD42 group has worked closely with all diamond manufacturers, most recently with II-VI Inc. [5] and Element Six Ltd. [6] to achieve improvements in charge collection and uniformity of pCVD diamond. This work has now resulted in large scale wafers of extremely high quality diamond. A summary of the present status of pCVD diamond is listed below:

- The charge collection distance of as-grown 12 cm diameter pCVD diamond wafers from production reactors now regularly exceeds 400 μm with a 5% uniformity across the wafer.
- Research pursued by RD42 in conjunction with II-VI Inc. yielded finished pCVD diamond material (500μm thick) with a collection distance of 300 μm.
- The radiation tolerance of high quality pCVD diamond has been tested up to 2×10^{16} p/cm^2.

Cleaning, surface preparation, preselection and testing are some of the most utilized functions RD42 provides to the CERN/LHC user community. We have the experience, expertise and facilities to dramatically help speed up a project (e.g. the CMS BCM1F upgrade). As was illustrated by the

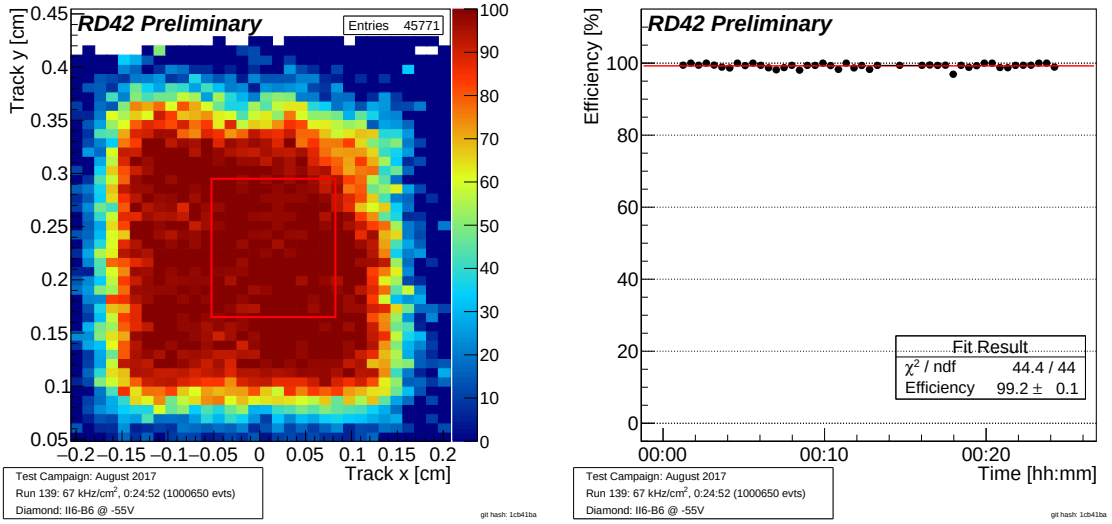

(a) (b)

Figure 6: The hit efficiency of the first 50μm $\times$ 50 μm cell pCVD 3D pixel detector with 3×2 ganged cells read out with CMS pixel electronics with a 1500e threshold. (a) shows the efficiency of each ganged cell as a function of xy position in the device. (b) shows the average efficiency in the fiducial region [the red box in (a)] as a function of time during the run at 67 kHz/cm^2.

RD42 collaborative effort with CMS, care in characterization and sensitivity to the critical issues is one of the keys to a successful detector. This is certainly true with silicon detectors as well. RD42 characterizes most, if not all, of the wafers grown for detector use and the final parts for selection. The characterization and processing techniques most often required before use are:

- Plasma processing to prepare the surface and remove any residual traps and defect from mechanical processing.
- Visible inspection with crossed polarizers and differential interference contrast to look for high stress regions, defects and voids.
- IV, CV with and without a source generating 20 nA of beam induced current to insure HV stability at high rates.
- Charge collection and MFP measurements at rates from 10 Hz to 10 kHz to ascertain the overall quality of the parts.

7 The Proposed RD42 Program

Due in large part to the pioneering work of many members of the RD42 collaboration and their continued leadership in diamond development, CVD diamond detector technology has developed from a mere concept to the point of playing a significant role in LHC experiments. We propose a program to further develop diamond devices, material and technologies so that they achieve significant charge collection, even after irradiations up to fluences of 10^{17} per cm^2. Further we propose to develop beam monitoring and pixel tracking prototypes based on 3D and sensor technology and characterise their performance: S/N, high voltage and current characteristics, efficiency and position resolution in beam tests over the course of the next three years. Each of the applications we have developed for use with pCVD and scCVD sensor material would have a larger signal-to-noise and work better with pCVD material configured with a 3D drift field and readout. Moreover, our collaboration possesses the unique experience with diamonds necessary to carry this program forward to this next stage of diamond detector development. If diamond detectors are to continue to under-pin beam monitoring, beam abort functionality, luminosity and expand their use into tracking applications at the HL-LHC and beyond it is crucial to perfect the production of 3D diamond sensors and understand their advantages and limitations in the next three years.

There are four aspects to our next 3 year program. First, we perfect the production of 3D electrode structures in diamond both with laser-processing techniques and, the more nascent, plasma techniques. We will endeavour to transfer the resulting technology to industry. Second, we will develop beam monitor prototypes based on pCVD sensors and test their performance up to the full fluences expected at the HL-LHC. This will put the LHC collaborations in a position to replace their beam protection and monitoring devices once, at the start of the HL-LHC running period and not have to track radiation induced damage effects throughout the LHC runs 4 and 5. Third, we will continue our materials work with manufacturers to advance the material quality and within RD42 to develop new techniques to measure and quantify any changes in material production. Progress in this area should translate directly into higher yield and thus reduced preselection, selection and production device times. This should allow CERN/LHC users to be able to test or use the best material if they decide they are interested in using diamond material. Fourth, we will develop pixel tracking prototypes using the RD53 readout chip and 3D diamond sensors and characterise their performance in beam tests after irradiation with fluences representative of inner tracking layers in ATLAS/CMS for run 5. This will put the experiments in a position to consider adopting 3D diamond pixel technology when it comes time to replace the inner tracking layers half way through the foreseen HL-LHC running period. In Fig. 7 we show the RD42 organization chart which indicates the six main focus areas in green and the sub-areas in orange which will facilitate the four aspects of the three year program described here.

7.1 3D Diamond Sensor Fabrication and Characterisation

The central point of our proposal is to build on our previous work. Our first main goal is to perfect the production of 3D diamond sensors. We are exploring two techniques for producing 3D columns electrodes through diamond material: laser processing of columns *one-by-one* or in small groups and traditional semi-conductor etching of small holes that are later filled with a conductive

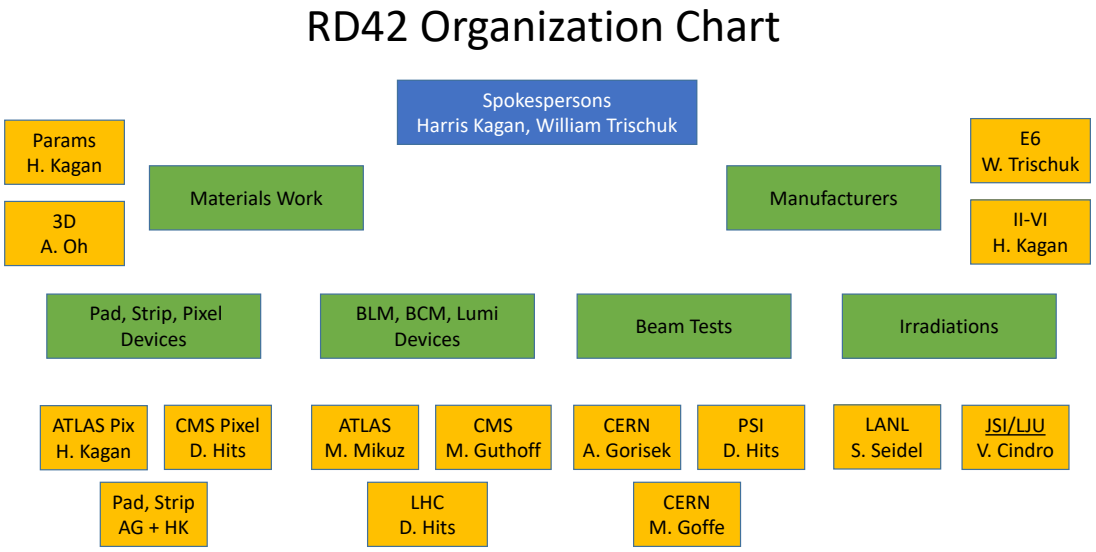

Figure 7: The RD42 Organization Chart indicating the areas of low level work and associated group leaders.

material. At this point the laser processing technique is more advanced and has allowed us to explore the patterning of bias grids and column readouts and the performance of relatively small areas of CVD diamond. We expect that etching techniques which are advancing rapidly to be scalable to larger areas than the laser technique.

In the next three years, we expect to concentrate on the following tasks:

- **Testbeam performance of 3D devices**. We are in the midst of characterising the performance: overall charge collection with 3D bias fields, the viability of the 3D cells in sensors that have been fabricated with 4000 (or more) cells, HV and I characteristics, inefficiencies for MIPs passing through the diamond in the vicinity of the 3D electrodes, charge sharing between 3D cells and ultimately the position resolution of tracking prototypes based on 3D diamond sensors.
- **Radiation Tolerance of 3D diamond devices**. We are just starting to expand the performance studies (described above) to 3D sensors that have been irradiated to typical HL-LHC fluences. In the coming year we expect to explore their performance after exposure to fluences of 10^{15}. Over the course of the next three years we will extend this to the ultimate fluences (10^{17}) for state-of-the-art (largest size) 3D diamond sensors.
- **Scaling the Laser processing techniques**. RD42 collaborators are continuing to pursue the scalability of the laser drilling techniques. They are exploring the use of wave-front modulation techniques that could allow the simultaneous production of O(10-20) electrode columns with a single pass of the laser. This would allow us to produce devices either 10-20$\times$ larger or 10-20$\times$ faster.
- **Plasma etching of holes to produce electrodes**. Other RD42 collaborators are beginning to explore the etching of small holes (less than 5 μm in diameter) and the subsequent filling of

these holes with conductive material to create the 3D bias and readout grid through the bulk of the diamond. The etching chambers have been fabricated and this work has begun.

7.1.1 Milestones

2019

- Complete testbeam analysis of early 3D prototypes to quantify HV and I operating points, charge collected, efficiency.
- Irradiation of two early 3D prototype sensors configured as pad detectors to 10^{15}.
- Laser drilling of 50 μm $\times$ 50 μm 3D cells with 2.5 μm diameter columns with $>$99.9% yield.
- First 3D columns from etching process produced and evaluated.

2020

- Testbeam studies of irradiated 3D sensors configured as pad detectors.
- Assess performance after 10^{15} fluences
- Scale up of 3D columns produced by laser and etching
- Irradiation of 50 μm $\times$ 50 μm cells to 10^{16}

2021

- Final scale of column production – produce 10 cm^2 sensors
- Testbeam studies of sensors irradiated to 10^{16}
- Transfer column production procedures to industry
- Irradiation to fluences of 10^{17}

7.2 HL-LHC Beam Monitoring Proof-of-Principle

All LHC experiments currently include diamond-based beam monitoring sensors with various readout granularities (both in space and time) [28, 29, 30]. Such devices will need to be improved for use during the HL-LHC era. At the same time, members of the RD42 collaboration have begun to study the use of diamond sensors at cryogenic temperatures with the goal of developing diamond-based beam loss monitors that could operate in the dipole cryostats (of the upgraded HL-LHC final focus triplets) enhancing the machine protection systems relative to the current baseline of gas-based BLM tubes.

In addition, we have learned a lot about the conflicting requirements of being able to set beam abort thresholds sufficiently high to avoid un-necessary loss of collision time while simultaneously remaining sensitive to MIPs from the collisions to be able to contribute to the measurement of the instantaneous luminosity being delivered. While part of this is down to the use of a wide range of readout gain, in conjunction with the radiation tolerance, part of it is simply making sensors that are less likely to change their charge response as they accumulate dose. We propose to

- **Make prototype beam loss detectors with planar and 3D diamond pad sensors**. Members of the RD42 collaboration are developing beam loss monitor readout chips based the 65 nm VLSI technology. At the same time they are addressing the factor of 10^4 to 10^5 difference in required sensitivity between beam abort incidents and luminosity measurements through a combination of the physical size/volume of diamond that is readout (smaller sensitive areas for MIPs/Lumi and larger areas for beam abort functionality) and the gain of the readout electronics that reads out the charge. It seems possible to get a factor of 30 (planar) to 100 (3D) in physical area, and still not be subject to non-linear charge collection from stray fields around the smallest readout pads and factors of 100 to 1000 in the gain of the readout electronics. The combination of these two approaches will be tested in prototypes that are being prepared now.
- **Characterise their performance up to 100 MHz MIP fluxes**. Once the prototypes are available we hope to be able to test them in a beam with particle fluxes approaching those present at the HL-LHC. Fluxes of 10-20 MHz are possible at PSI. To go beyond this would require setting up a test in one of the LHC caverns, at the start of Run 3.
- **Demonstrate stable performance after fluences of** 10^{17}. Finally we will want to irradiate one or more of our beam monitor packages up to fluences well beyond 10^{16} to demonstrate the robustness of the technical solutions chosen for operation of a single set of beam monitor sensors throughout the HL-LHC era (Runs 4 and 5).

7.2.1 Milestones

2019

- Produce the first RD42 65 nm HL-LHC beam loss/lumi chip
- Assemble first HL-LHC beam loss monitor station
- Test at PSI with fluxes up to 20 MHz
- Irradiate one station to a fluence of 10^{15}

2020

- Production HL-LHC beam loss readout chip
- Test un-irradiated beam loss station with production chip in beam at CERN
- Test irradiated beam loss station (from previous year) with MIPs at CERN
- Irradiate one station to a fluence of 10^{16}

2021

- Work with manufacturers to produce pCVD diamond for HL-LHC systems
- Preselect, metalise diamond for the ATLAS BCM' project (and similar for CMS)
- Beam test of BCM' modules using the RD42 65 nm chip

7.3 Development of pCVD Material

All of the above areas would benefit with better material. Manufacturers are interested in working with RD42 to give them feedback on their production techniques. The most recent example of this effort yielded the plasma processing step that is used on all pCVD material to remove any residual traces of the mechanical processing steps routinely used in CVD diamond production. Moreover RD42 is in the process of developing new techniques for more detailed information about the internal electric field in the material. Finally there is data which indicates that given a fixed amount of CVD growth time, slower growth will yield thinner but higher quality material (less defects, larger collected charge, better high voltage and current characteristics). Historically, progress in any of these would dramatically reduce the preselection and selection testing required to construct a useful device.

7.3.1 Milestones

2019

- Develop edge-TCT to measure the internal electric field configuration of CVD material.
- Work with manufacturers to reduce the surface imperfections and voids to less than 1/cm^2.

2020

- Work with manufacturers to produce the first pCVD material with 400 μm collection distance in a finished part 500 μm thick.

2021

- Work with manufacturers to reduce the as-grown charge collection distance uniformity across a 12 cm wafer to $< 2\%$.

7.4 Development of 3D Diamond Pixel Module Prototypes

The innermost devices at the HL-LHC will have to withstand enormous fluxes. This means that eventually all innermost devices will be driven to pixel geometries. RD42 has already sucessfully produced 50 μm $\times$ 50 μm 3D cells and tested them with present generation pixel electronics by ganging them in a 3 $\times$ 2 readout configuration. Our goal in this section is to test and characterise these small cell pixel devices with the RD53 prototype chip.

- **Fabricate and characterize a number of new 50 μm $\times$ 50 μm 3D diamond pixel devices with >99% yield and test them with the RD53 prototype pixel electronics** The methodology for producing pCVD 3D pixel devices is progressing well but we have not tested many with the most recent advances nor have we irradiated them. To get to the next level of reliability this must be completed.
- **Fabricate 25 μm $\times$ 25 μm pixel cells and compare them with 50 μm $\times$ 50 μm cells**. The signal size of 3D diamond device is a critical issue. It may be necessary to go to 25 μm $\times$ 25 μm cells to actually reach the efficiency required at 10^{17} hadrons/cm^2. Thus we propose to fabricate 25 μm $\times$ 25 μm 3D pixel cells and test them with the RD53 prototype pixel chip. This will involve 2 $\times$ 2 ganging to use the same electronics.

- **Irradiate the new pCVD 3D pixel devices with all the latest advances up to 10^{17} hadrons/cm^2** One of our primary successes of the past few years was to quantify the radiation tolerance of pCVD and scCVD diamond material. Another lesson we learned was that new material must be tested to confirm the previous results. It is critical to quantify the fluence the pCVD 3D diamond detectors will survive in order to support proposals for their use at the HL-LHC. If they are really as radiation tolerant as expected many new areas of use will be proposed.

7.4.1 Milestones

2019

- Fabricate and characterize a number of 3D diamond pixel devices with the latest advances with 50 μm $\times$ 50 μm cell size.
- Irradiate a small number of these 3D diamonds pixel devices up to 10^{15}/cm^2.
- Characterise radiation tolerance of 3D pixel devices in beam tests with the RD53 chip.

2020

- Fabricate and characterize a number of 3D diamond pixel devices with the latest advances with 25 μm $\times$ 25 μm cell size.
- Irradiate a small number of these 3D diamonds pixel devices up to 10^{16}/cm^2.
- Directly compare the 25 μm cells with the 50 μm cells in a beam test.

2021

- Confirm radiation hardness of 3D diamond devices in beam tests up to 10^{17} hadrons/cm^2.
- Technology transfer.
- Construct and test pCVD diamond pixel based beam monitoring devices.

8 Summary

The recent progress in the design, fabrication and testing of pCVD diamond detectors was presented. The following milestones have been achieved: successful operation of the first pCVD diamond planar pixel detector in the ATLAS experiment at the LHC; demonstration that the average signal pulse height of pCVD diamond detectors irradiated up to 4×10^{15} n/cm^2 is independent of the particle flux up to $\sim$20 MHz/cm^2; successful fabrication and operation of the first pCVD diamond 3D pixel detector with 50 μm $\times$ 50 μm pixels read out with CMS pixel electronics where the efficiency for a MIP was $>$99% and the average charge collected in the device was $>$90% of the deposited charge. The future RD42 plans were presented with milestones to continue this work up to doses up to 10^{17} n/cm^2 and continue the development of 3D diamond detectors with the 50 μm $\times$ 50 μm and 25 μm $\times$ 25 μm cell sizes in pCVD diamond.

References

[1] W. Adam, *et al.* [RD42 collaboration], *Development of Diamond Tracking Detectors for High Luminosity Experiments at the LHC*, Proposal/RD42 CERN/DRDC 94-21, Status Report/RD42, CERN/LHCC, 95-43, 95-53, 95-58, 97-03, 98-20, 2000-011, 2000-015, 2001-002, 2002-010, 2003-063, 2005-003, 2006-010, 2007-002, 2008-005.

[2] M. Artuso, *et al.* [RD42 Collaboration], *RD42 Status Report: Development of Diamond Tracking Detectors for High Luminosity Experiments at the LHC*, CERN-LHCC-2017-006.

[3] G. Apollinari, *et al.*, *High-Luminosity Large Hadron Collider (HL-LHC): Technical Design Report V.0.1*, CERN Yellow Reports: Monographs, Volume 4/2017 CERN-2017-007-M, CERN Geneva 2017, https://doi.org/10.23731/CYRM-2017-004.

[4] PSI High Intensity Proton Accelerator, *High Energy Beam Lines*, http://www.psi.ch/abe/high-energy-beam-lines

[5] II-VI Inc., 360 Saxonburg Road, Saxonburg, PA.

[6] Element Six Ltd., King's Ride Park, Ascot, Berkshire SL5 9BP UK; Diamond Detector Ltd., 16 Fleetsbridge Business Centre, Upton Road, Poole, Dorset BH17 7AF UK.

[7] F. Bachmair, *CVD Diamond Sensors In Detectors For High Energy Physics*, Ph.D. Thesis, ETH Zürich (2016), https://doi.org/10.3929/ethz-a-010748643.

[8] Y. Allkofer, *et al.* [CMS Experiment], "Design and performance of the silicon sensors for the CMS barrel pixel detector," Nucl. Instrum. Meth. Phys. Res. A **584** (2008) 25.

[9] H.Chr. Kästli, *et al.*, *Design and performance of the CMS pixel detector readout chip*, Nucl. Instrum. Meth. Phys. Res. A **565** (2006) 188.

[10] S. Ritt, *DRS4 Evaluation Board*, http://www.psi.ch/drs/evaluation-board

[11] P. W. Lisowski and K. F. Schoenberg, *The Los Alamos Neutron Science Center*, Nucl. Instrum. Meth. Phys. Res. A **562** (2006) 910.

[12] K. Ishii et al., *Cyric annual report 2010-2011*, 1, 2012.

[13] L. Snoj, G. Žerovnik, and A. Trkov, *Computational analysis of irradiation facilities at the JSI TRIGA reactor*, Appl. Radiat. and Isot. **70.3** (2011) 483.

[14] Integrated Detectors & Electronics AS, Data Sheet VA2 Readout Chip, Oslo, Norway, 2014.

[15] L. Bäni, *Top Quarks and Diamonds*, Ph. D. Thesis, ETH Zürich (2017), https://doi.org/10.3929/ethz-b-000222412.

[16] D. Meier et al., [RD42 Collaboration], *Proton Irradiation of CVD Diamond Detectors for High Luminosity Experiments at the LHC*, Nucl. Instrum. Meth. Phys. Res. A **426** (1999) 173.

[17] D. Asner et al., [RD42 Collaboration], *Diamond pixel modules*, Nucl. Instrum. Meth. Phys. Res. A **636** (2011) S125.

[18] G. Aad, *et al.* [ATLAS collaboration], *The ATLAS experiment at the CERN Large Hadron Collider*, JINST **3** S08003, 2008.

[19] M. Červ, *et al.*, *The ATLAS Diamond Beam Monitor*, JINST **9** C02026, 2014.

[20] M. Barbero, *et al.*, *The FE-I4 pixel readout chip and the IBL module*, PoS(Vertex 2011) **038** (2011).

[21] A.J. Edwards, *et al.*, *Radiation monitoring with diamond sensors in BABAR*, IEEE Trans. Nucl. Sci. **51** (2004) 1808.

[22] F. Huegging, *et al.* [ATLAS Collaboration], *The ATLAS Pixel Insertable B-Layer (IBL)*, Nucl. Instrum. Meth. Phys. Res. A **650** (2011) 45.

[23] S. Parker, C.J. Kenney and J. Segal, *3-D: A proposed new architecture for solid state radiation detectors*, Nucl. Instrum. Meth. Phys. Res. A **395** (1997) 328.

[24] F. Bachmair, *et al.* [RD42 Collaboration], *A 3D Diamond Detector for Particle Tracking*, Nucl. Instrum. Meth. Phys. Res. A, **786** (2015) 97.

[25] A. Alexopoulos, *et al.* [RD42 Collaboration], *Diamond detector technology: status and perspectives*, PoS(Vertex 2016) **027** 2016.

[26] M. Garcia-Sciveres, *et al.* [RD53 Collaboration], *The RD53A Integrated Circuit*, CERN-RD53-PUB-17-001 (2017). https://cds.cern.ch/record/2287593?ln=en.

[27] S. Zhao, *Characterization of the Electrical Properties of Polycrystalline Diamond Films'*, Ph.D. Dissertation, Ohio State University (1994).

[28] V. Cindro *et al.* [ATLAS], *The ATLAS Beam Conditions Monitor*, JINST **3**, 02004 (2008).

[29] E. Bartz, *et al.* [CMS], *The PLT: A Luminosity Monitor for CMS Based on Single-Crystal Diamond Pixel Sensors*, Nucl. Phys. B (Proc. Suppl.) **197**, 171 (2009).

[30] M. Domke, *et al.* [LHCb], *Commissioning of the beam conditions monitor of the LHCb experiment at CERN*, 2008 IEEE Nuclear Science Symposium Conference Record **N58-6**, 3306 (2008).

[31] R. Wallny, *et al.* [RD42 Collaboration], *Beam test results of the dependence of signal size on incident particle flux in diamond pixel and pad detectors*, JINST **10 C07009** (2015).